Materials Science & Engineering A 589 (2014) 271–274

Contents lists available at ScienceDirect

Materials Science & Engineering A

journal homepage: www.elsevier.com/locate/msea

Rapid communication

Achieving friction stir welded SiCp/Al–Cu–Mg composite joint of nearly equal strength to base material at high welding speed

D. Wang [a,b], Q.Z. Wang [b], B.L. Xiao [b], Z.Y. Ma [b,*]

[a] University of Science and Technology of China, 96 Jinzhai Road, Hefei 230026, China
[b] Shenyang National Laboratory for Materials Science, Institute of Metal Research, Chinese Academy of Sciences, 72 Wenhua Road, Shenyang 110016, China

ARTICLE INFO

Article history:
Received 8 June 2013
Received in revised form
25 September 2013
Accepted 27 September 2013
Available online 4 October 2013

Keywords:
Friction stir welding
Metallic composites
Microstructure
Mechanical properties

ABSTRACT

Three-millimeter-thick 17 vol%SiCp/2009Al-T4 plates were successfully friction stir welded. The ultimate tensile strength of the joints increased as the welding speed increased from 50 to 800 mm/min and reached 97% of the base material at 800 mm/min, with the fracture location shifting from the first low-hardness zone adjacent to the nugget zone to the nugget zone.

1. Introduction

Friction stir welding (FSW), a solid-state joining technique, is considered a promising welding method for joining discontinuously reinforced aluminum matrix composites (AMCs), which avoid the drawbacks of fusion welding [1,2]. In recent years, a number of investigations have been conducted to join AMCs by FSW [3–9]. The sound joints of the AMCs with different reinforcements, such as SiC, Al_2O_3, B_4C, TiB_2 and ZrB_2, could be achieved by FSW [5–9]. High joint efficiencies of 70% to 87% could be obtained in the joints. Similar to the FSW joints of heat-treatable Al alloys [10,11], the FSW joints of heat-treatable AMCs exhibit the lowest hardness in the heat-affected zone (HAZ), owing to the dissolution and coarsening of the precipitates during FSW. This results in that the FSW AMC joints usually failed in the HAZ. Therefore, the strength of the joints is usually determined by the hardness of the low-hardness zone of the HAZ.

The hardness of the HAZ could be increased by increasing the welding speed for heat-treatable Al alloys and AMCs [10,12,13]. However, for AMCs, the highest welding speed reported was 300 mm/min [4,6], with some defects detected on the bottom of the nugget zone (NZ). The critical factor that restricts the welding speed of AMCs is the severe wear of the FSW tool owing to the presence of hard ceramic reinforcements [12,14]. In our previous study, an ultra-hard material tool was used to join 15 vol%SiCp/2009Al-T4 plates [15]; such a cylindrical tool without threads exhibited almost no wear in FSW.

In this study, the tool was machined into a threaded conical shape to enhance the material flow during FSW, and 17 vol%SiCp/2009Al-T4 composite plates were subjected to an investigation of FSW at high welding speed. The aims are to investigate the possibility of joining SiCp/2009Al-T4 at high welding speed and to increase the mechanical properties of the FSW joints.

2. Material and methods

Plates of 3-mm-thick 17 vol%SiCp/2009Al composite were used in this study. 2009Al had a nominal chemical composition of Al–4.26Cu–1.61Mg (wt%) and SiC particles had an average size of 7 μm. The composite was subjected to T4 temper (solutionized at 516 °C for 1 h, water quenched, and naturally aged for 7 days). The plates were friction stir butt welded along the rolling direction at a tool rotation rate of 1000 rpm and welding speeds of 50, 200, and 800 mm/min. The samples were named: FSW-50, FSW-200, and FSW-800, respectively. An ultra-hard cermet tool with a shoulder 14 mm in diameter and a threaded conical-shaped pin 5 mm in diameter and 2.9 mm in length was used. After welding, the joints were aged naturally for 7 days.

Optical microscopic (OM) examination and hardness measurements were carried out on the cross-section of the joints perpendicular to the welding direction. The Vickers hardness profiles of the joints were measured along the mid-thickness of the welded plate using an automatic testing machine (LECO, LM-247AT) under a load of 500 g for 13 s. Tensile specimens with a gauge length of 40 mm and a width of 10 mm were machined perpendicular to the welding direction with the NZ being in the center of the gauge.

* Corresponding author. Tel./fax: +86 24 83978908.
E-mail address: zyma@imr.ac.cn (Z.Y. Ma).

0921-5093/$ - see front matter © 2013 Elsevier B.V. All rights reserved.
http://dx.doi.org/10.1016/j.msea.2013.09.096

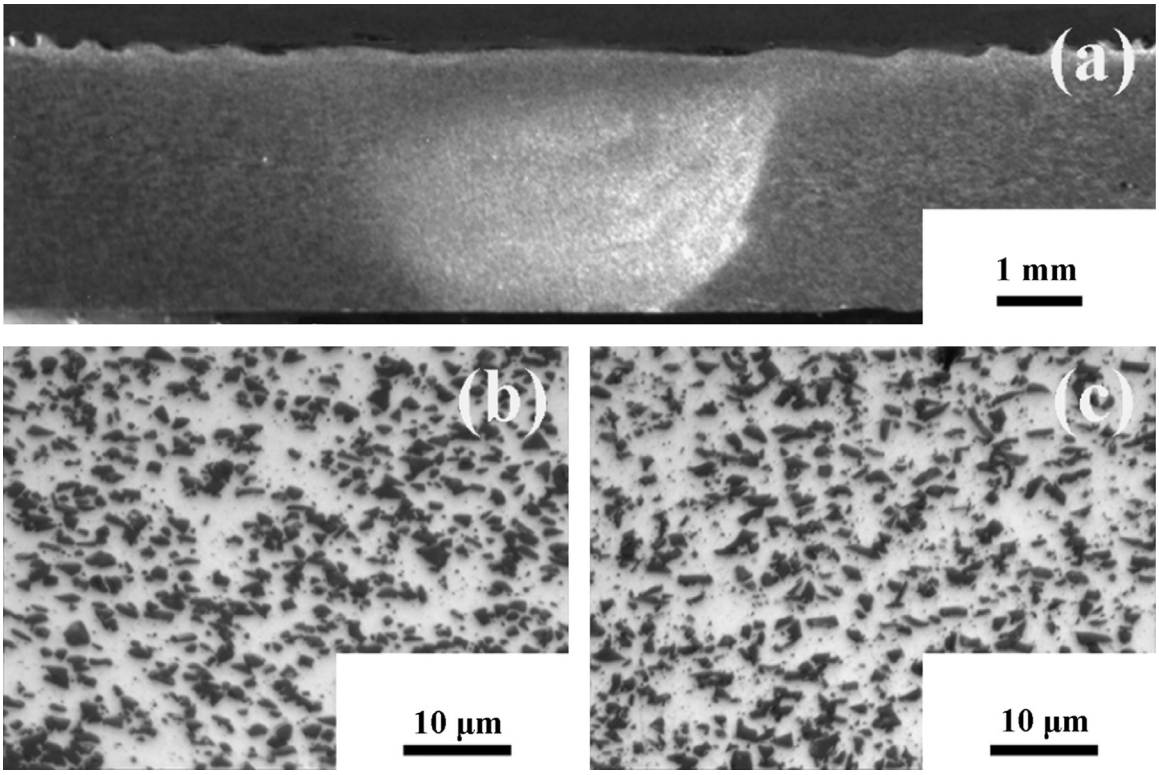

Fig. 1. Optical images of FSW SiCp/2009Al joint at 800 mm/min: (a) macrostructure of joint, (b) base material, and (c) nugget zone.

The precipitation of the joints and based material (BM) were analyzed by transmission electron microscopy (TEM, Phillip TECNAI F20).

3. Results and discussion

Fig. 1a shows a macrograph of the FSW-800 sample. No defects were observed in the joint, indicating that a sound joint could be achieved by FSW at a high welding speed of 800 mm/min. Similarly, sound joints were produced at welding speeds of 50 and 200 mm/min (not shown). Because this study focuses on high welding speeds, the FSW-800 sample was subjected to detailed examination of its microstructure. Fig. 1b and c shows the optical microstructure of the BM and the NZ of the FSW-800 sample perpendicular to the welding direction, respectively. The SiC particles in the NZ were distributed homogeneously, similar to that in the BM.

Fig. 2 shows the hardness profiles of the joints at various welding speeds. At a welding speed of 50 mm/min, two low-hardness zones were observed in the HAZ on both advancing and retreating sides, similar to that seen in Al–Cu–Mg alloys at low welding speed [11,16]. The first low-hardness zone adjacent to the NZ had the lowest hardness. When the welding speed increased to 200 mm/min, the hardness value of the HAZ increased significantly compared with that at 50 mm/min. Two low-hardness zones were still observed in each HAZ. At a higher welding speed of 800 mm/min, the NZ exhibited the lowest hardness (~160 Hv) and each HAZ contained only one low-hardness zone.

Table 1 shows that the ultimate tensile strength (UTS) of the FSW joints increased as the welding speed increased. At the high welding speed of 800 mm/min, the joint efficiency reached 97%, which was higher than that reported previously for FSW AMCs [3–6]. The FSW-50 and FSW-200 samples failed in the first low-hardness zone adjacent to the NZ, whereas the FSW-800 sample fractured in the NZ, which was consistent with the lowest hardness distribution.

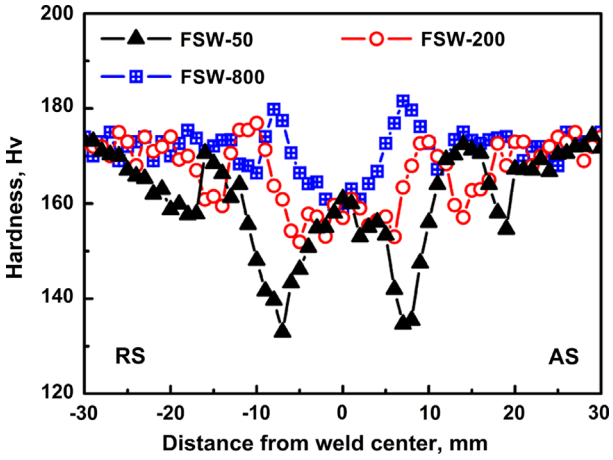

Fig. 2. Hardness profiles of FSW SiCp/2009Al joints.

Table 1
Tensile properties of SiCp/2009Al composite joints.

Sample	YS, MPa	UTS, MPa	Elongation, %	Joint efficiency, %
BM	344 ± 5	514 ± 4	4.0 ± 0.5	–
FSW-50	316 ± 10	419 ± 2	3.0 ± 0.2	82
FSW-200	339 ± 1	479 ± 4	3.5 ± 0.2	93
FSW-800	341 ± 7	501 ± 2	3.5 ± 0.1	97

Fig. 3a shows the TEM image of the BM. Many dislocations were observed in the matrix and no precipitates were detected. The selected area electron diffraction (SAED) pattern in the Al

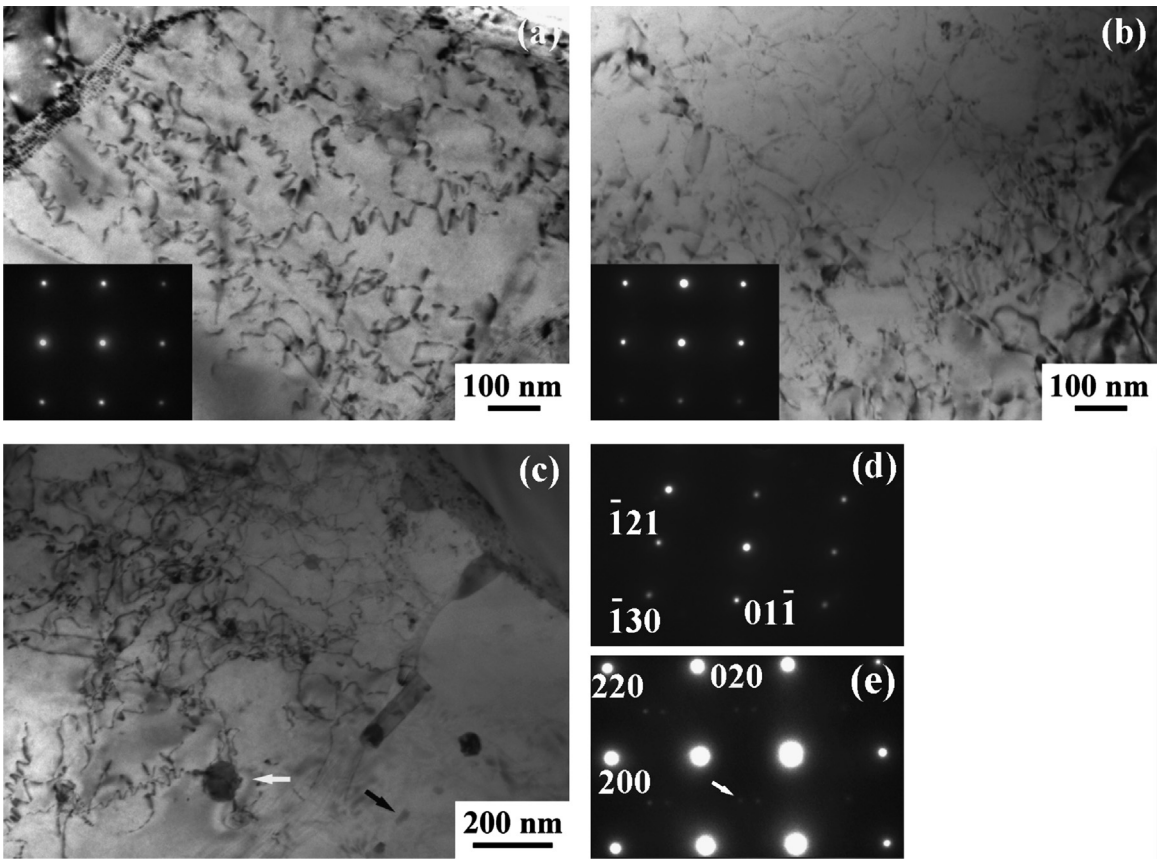

Fig. 3. TEM micrographs of FSW SiCp/2009Al joint at 800 mm/min: (a) base material, (b) low-hardness zone of HAZ, (c) nugget zone, (d) SAED pattern of Al_2Cu phase, marked by white arrow in Fig. 3c, and (e) SAED pattern in the Al matrix ⟨100⟩ projection (region marked by black arrow in Fig. 3c).

matrix ⟨100⟩ projection (insert in Fig. 3a) only contained the diffraction spots of Al matrix, indicating that no GP zones were present in the Al matrix. For the SiCp/2009Al, the composite was strengthened by the clusters of solute atoms [17,18], when the composite was under natural aging temper. Therefore, no other diffraction spots were observed in the SAED pattern of the BM.

Fig. 3b shows the TEM image of the low-hardness zone in the HAZ of the FSW-800 sample. Similar to that in the BM, no precipitate was detected in the low-hardness zone under TEM, and meanwhile, no diffraction spots of the GP zones were observed in the SAED pattern (insert in Fig. 3b). Fig. 3c illustrates the TEM image of the NZ of the FSW-800 sample. The circular θ phase (proved by the SAED pattern (Fig. 3d)) with a size of ~100 nm were observed in the Al matrix, marked by the white arrow. Furthermore, small irregular phases with a size of ~20 nm, indicated by the black arrow, were also observed in the Al matrix. In the SAED pattern, around the small phase in the Al matrix ⟨100⟩ projection (Fig. 3e), weak diffraction spots, marked by the white arrow, were associated with the S phase [18]. This means that both θ and S phases generated in the NZ during FSW.

Jariyaboon et al. [19] found that the temperature adjacent to the NZ was 480 °C during FSW of 2024Al-T351 alloy. Similarly, Fu et al. [13] reported that the peak temperature adjacent to the NZ in FSW of 1.6 mm 2024Al-T3 alloy at a welding speed of 1000 mm/min was about 450 °C and that it took only 1.5 s to reduce the temperature from 450 to 200 °C. Therefore, for the FSW-800 sample, the peak temperature of the NZ during FSW was possibly similar to the above temperatures. During the cooling process following FSW, the θ phase would first precipitate in the Al matrix. As the temperature decreased further, the precipitation of the S phases was facilitated. Meanwhile, the short thermal cycle of FSW resulted in the small size of the θ and S phases.

In this study, at low welding speeds of 50 and 200 mm/min, two low-hardness zones were observed in the HAZ on both advancing and retreating sides. Similar to the results of the FSW Al–Cu–Mg alloys [10,11], the HAZ of the joints had the lowest hardness owing to the dissolution and coarsening of the precipitates. However, at 800 mm/min, the high welding speed resulted in a much-shortened length of thermal exposure in the HAZ during FSW. In this case, only part of the clusters dissolved into the Al matrix in the HAZ. Therefore, this region had the similar microstructure to the BM under TEM (Fig. 3b), resulting in that the hardness of the HAZ was higher than that of the NZ. This increases the strength of the joint significantly to nearly be equal to that of the base material, with the fracture location shifting from the first low-hardness zone to the nugget zone.

4. Conclusions

FSW joints of 3 mm-thick 17 vol%SiCp/2009Al-T4 composite were successfully achieved using a threaded cermet tool at a tool rotation rate of 1000 rpm and welding speeds of 50, 200 and 800 mm/min. At low welding speeds of 50 and 200 mm/min, two low-hardness zones were observed in the heat-affected zones. By increasing the welding speed to 800 mm/min, the first low-hardness zone adjacent to the nugget zone disappeared and the nugget zone exhibited the lowest hardness. As the welding speed increased, the ultimate tensile strength of the joints increased and the fracture location shifted from the first low-hardness zone to the nugget zone. The strength of the joint at 800 mm/min reached up to 97% of the base material.

Prime novelty statement

Three millimeter thick 17 vol%SiCp/2009Al-T4 plates were successfully friction stir welded using a threaded cermet tool. As the welding speed increased, the ultimate tensile strength of the joints increased and the fracture location shifted from the first low-hardness zone to the nugget zone. The strength of the joint at 800 mm/min reached up to 97% of the base material.

Acknowledgments

The authors gratefully acknowledge the support of the National Basic Research Program of China under Grant no. 2012CB619600 and the National Natural Science Foundation of China under Grant no. 51331008.

References

[1] R.S. Mishra, Z.Y. Ma, Materials Science and Engineering R 50 (2005) 1–78.
[2] D. Storjohann, O.M. Barabash, S.S. Babu, S.A. David, P.S. Sklad, E.E. Bloom, Metallurgical and Materials Transactions A 36 (2005) 3237–3247.
[3] G. Minak, L. Ceschini, I. Boromei, M. Ponte, International Journal of Fatigue 32 (2010) 218–226.
[4] L. Ceschini, I. Boromei, G. Minak, A. Morri, F. Tarterini, Composites Science and Technology 67 (2007) 605–615.
[5] A.H. Feng, B.L. Xiao, Z.Y. Ma, Composites Science and Technology 68 (2008) 2141–2148.
[6] L.M. Marzoli, A.V. Strombeck, J.F.D. Santos, C. Gambaro, L.M. Volpone, Composites Science and Technology 66 (2006) 363–371.
[7] X.G. Chen, M.D. Silva, P. Gougeon, L.S. Georges, Materials Science and Engineering A 518 (2009) 174–184.
[8] S.J. Vijay, N. Murugan, Materials Design 31 (2010) 3585–3589.
[9] I. Dinaharana, N. Muruganb, Materials Science and Engineering A 543 (2012) 257–266.
[10] F.C. Liu, Z.Y. Ma, Metallurgical and Materials Transactions A 39 (2008) 2378–2388.
[11] M.J. Jones, P. Heurtier, C. Desrayaud, F. Montheillet, D. Allehaux, J.H. Driver, Scripta Materialia 52 (2005) 693–697.
[12] M.S. Khorrami, M. Kazeminezhad, A.H. Kokabi, Materials Science and Engineering A 543 (2012) 243–248.
[13] R.D. Fu, J.F. Zhang, Y.J. Li, J. Kang, H.J. Liu, F.C. Zhang, Materials Science and Engineering A 559 (2013) 319–324.
[14] R.A. Prado, L.E. Murr, D.J. Shindo, K.F. Sota, Scripta Materialia 45 (2001) 75–80.
[15] D. Wang, B.L. Xiao, Q.Z. Wang, Z.Y. Ma, Materials Design 47 (2013) 243–247.
[16] C. Genevois, A. Deschamps, A. Denquin, B.D. Cottignies, Acta Materialia 538 (2005) 2447–2458.
[17] P. Rodrigo, P. Poza, V. Utrilla, A. Urena, Journal of Alloys and Compounds 479 (2009) 451–456.
[18] R.K.W. Marceau, G. Sha, R.N. Lumley, S.P. Ringer, Acta Materialia 58 (2010) 1795–1805.
[19] M. Jariyaboon, A.J. Davenport, R. Ambat, B.J. Connolly, S.W. Williams, D.A. Price, Corrosion Science 49 (2007) 877–909.